Experimental and materials considerations for the topological superconducting state in electron- and hole-doped semiconductors: Searching for non-Abelian Majorana modes in 1D nanowires and 2D heterostructures

Jay D. Sau,[1,*] Sumanta Tewari,[2] and S. Das Sarma[1]

[1]*Condensed Matter Theory Center and Joint Quantum Institute, Department of Physics, University of Maryland, College Park, Maryland 20742-4111, USA*

[2]*Department of Physics and Astronomy, Clemson University, Clemson, South Carolina 29634, USA*

(Received 16 November 2011; published 14 February 2012)

In proximity to an s-wave superconductor, a one- or two-dimensional, electron- or hole-doped semiconductor with a sizable spin-orbit coupling and a Zeeman splitting can support a topological superconducting (TS) state. The semiconductor TS state has Majorana fermions as localized zero-energy excitations at order parameter defects such as vortices and sample edges. Here we examine the effects of quenched disorder from the semiconductor surface on the stability of the TS state in both electron- and hole-doped semiconductors. By considering the interplay of broken time-reversal symmetry (due to Zeeman splitting) and disorder we derive an expression for the disorder suppression of the superconducting quasiparticle gap in the TS state. We conclude that the effects of disorder can be minimized by increasing the ratio of the spin-orbit energy with the Zeeman splitting. By giving explicit numbers we show that a stable TS state is possible in both electron- and hole-doped semiconductors for experimentally realistic values of parameters. We discuss possible suitable semiconductor materials which should be the leading candidates for the Majorana search in solid state systems.

DOI: 10.1103/PhysRevB.85.064512 PACS number(s): 03.67.Lx, 71.10.Pm, 74.45.+c

I. INTRODUCTION

In a recent paper[1] it has been shown that a 2D spin-orbit-coupled electron-doped semiconductor, in proximity to a bulk s-wave superconductor and an externally induced Zeeman splitting, can support a topological superconducting phase with Majorana fermion modes at vortex cores and sample edges, i.e., at order parameter defect locations. It has also been realized from dimensional reduction that the edge Majorana modes in a sample with rectangular geometry (of width W) turn into localized *end* Majorana modes in the corresponding 1D geometry ($W \to 0$) and, further, in 1D the excitation gap above the Majorana modes (minigap) should scale as the induced superconducting gap Δ [thus avoiding the problem of a tiny minigap, $\Delta^2/\epsilon_F \sim 0.1$ mK, as in 2D $(p_x + ip_y)$-wave superconductors]. The end Majorana modes in the 1D geometry should be experimentally visible in local zero-bias tunneling experiments. These results, numerically confirmed soon thereafter,[2] have appeared with analytical and numerical details for both 1D and 2D semiconductors in Ref. 3. It has also been pointed out[4,5] that the required Zeeman splitting in 1D can be induced by a magnetic field parallel to the adjacent superconductor (thus avoiding the problem of orbital effects[6]), and the non-Abelian character of the end Majorana modes can be probed by Josephson experiments. Very recently it has been shown that the generic Luttinger Hamiltonian applicable to the *hole-doped* nanowires also supports end Majorana modes[7] in a manner similar to its electron-doped counterpart. The 1D electron- or hole-doped wires in the TS state can be arranged in a quasi-1D network geometry[8] to test non-Abelian statistics[8] and perform topological quantum computation (TQC)[9,10] in the Bravyi-Kitaev (BK) scheme.[11] In principle, TQC in the BK scheme is also possible with the 2D semiconductor TS states using Majorana fermion interferometry[12] analogous to that in the $\nu = 5/2$ fractional quantum Hall (FQH) states,[13] chiral p-wave superconductors,[14] and TS states on the surface of topological insulators.[15,16] Efforts to realize a semiconductor TS state with Majorana fermions in proximity to s-wave superconductors are currently underway in many laboratories worldwide, concentrating on both 1D semiconducting nanowires and 2D semiconductor heterostructures in close proximity to a regular bulk s-wave superconductor (e.g., Al, Nb).

In view of the ongoing experimental efforts on semiconductor TS states, it is important to understand the effects of disorder from the semiconductor surface on the realizability of the TS state. (In recent works[17] it has been established that the disorder residing in the adjacent bulk superconductor has negligible effect on the semiconductor TS state, and therefore in this paper we will ignore the effects of disorder from the bulk superconductor.) This is an especially important question[18–20] because the TS states in semiconductors explicitly break the time reversal (TR) symmetry and it is known that the superconducting quasiparticle gap in such systems, unlike that in TR-invariant superconductors,[21] is suppressed by disorder. Below we will measure the extent of TR breaking in the semiconductor TS state (in both 1D and 2D) by the ratio $r = V_Z/(\alpha k_F)$, where V_Z is the Zeeman energy in the TS state and αk_F gives the typical spin-orbit energy scale (with α as the Rashba spin-orbit coupling constant). We will show that the disorder suppression of the superconducting quasiparticle gap from its clean value increases with increasing values of r. Nonetheless, by giving explicit numbers we show that a reasonable TS state quasiparticle gap can be experimentally achievable in both electron- and hole-doped systems even in the presence of realistic disorder. For electron-doped wires we find that with a mobility of $\sim$100 000 cm^2/V-s a measurable robust TS state gap of 50–100 mK is achievable. We also find that for hole-doped wires with a significantly larger spin-orbit

energy $E_{\rm SO} \sim 30$ meV,[22,23] a larger gap of 0.8 K is achievable for a mobility of $\sim$100 cm^2/V-s.

In what follows, by Δ_s we denote the quasiparticle gap (pair potential) in the (proximity-inducing) bulk superconductor. For the semiconductor (2D or 1D), α is the Rashba spin-orbit coupling constant, m^* is the effective mass (of electrons or holes), V_Z is the Zeeman splitting required for the TS state, Δ_0 is the proximity-induced pair potential, Δ is the quasiparticle gap at the Fermi surface, k_F is the Fermi momentum ($\hbar = e = k_B = 1$), and $1/\tau_{sm}$ is the effective intrinsic semiconductor disorder scattering rate. In the semiconductor, the combination of the Zeeman splitting and the spin-orbit coupling results in a Fermi-surface quasiparticle gap Δ, which differs from the proximity-induced pair potential Δ_0, and thus we have three distinct superconducting gaps Δ_s, Δ, and Δ_0 to consider in this problem.

In Sec. II we first give our starting Hamiltonian for the semiconductor which includes a proximity-induced pair potential, an externally applied Zeeman splitting, and a disorder potential. We then calculate the dependence of the disordered TS state quasiparticle gap on the semiconductor disorder scattering rate $1/\tau_{sm}$ [Eq. (18)].

In Sec. III, we review the two systems that we will apply our results to, namely, electron- and hole-doped semiconductors. In Sec. IV, we use the results of Secs. II and III to give explicit realistic values for the various parameters for a stable TS state in electron-doped semiconductors.

This is followed by the case of hole-doped semiconductors, where again using explicit values of the parameters we show that a stable TS state is possible. We find that the TS state gap in the hole-doped case can be much larger and more robust to disorder effects than in its electron-doped counterpart due to larger values of α and m^*. We conclude in Sec. V with a summary and an outlook with a detailed qualitative discussion on why the key problem of choosing the optimal materials combination for realization of the TS state is experimentally important.

II. BdG HAMILTONIAN WITH DISORDER

The BdG Hamiltonian in real space for spin-1/2 electrons with spin-singlet pairing potential is written as

$$H_{\rm BdG} = \begin{pmatrix} H_{sm} - \epsilon_{F,sm} & \Delta_0 \\ \Delta_0 & \epsilon_{F,sm} - \sigma_y H_{sm}^* \sigma_y \end{pmatrix}, \qquad (1)$$

where Δ_0 is a real, constant, s-wave spin-singlet pairing potential in the semiconductor which is proximity induced from an adjacent superconductor, $H_{sm} \equiv H_{sm}(\boldsymbol{r},\sigma;\boldsymbol{r}'\sigma')$ is the noninteracting part of the semiconductor Hamiltonian with disorder, and $\epsilon_{F,sm}$ is the chemical potential. Here $\sigma_{x,y,z}$ are the Pauli matrices. For a disordered semiconductor, with spatially localized (i.e., short-ranged) spin-independent disorder, H_{sm} can be written as

$$H_{sm}(\boldsymbol{r},\sigma;\boldsymbol{r}'\sigma') = H_{sm,\rm clean}(\boldsymbol{r},\sigma;\boldsymbol{r}'\sigma') + V(\boldsymbol{r})\delta(\boldsymbol{r}-\boldsymbol{r}')\delta_{\sigma\sigma'}, \qquad (2)$$

where $V(\boldsymbol{r})$ is the local potential induced by disorder.

In the limit of weak disorder and weak pairing where both $V(\boldsymbol{r})$ and Δ_0 are smaller than the interband spacing of the spin-orbit bands in the semiconductor, it is convenient to work in the basis of Bloch eigenstates $|n,k\rangle$ of $H_{sm,\rm clean}(\boldsymbol{r}\sigma;\boldsymbol{r}'\sigma')$. In particular, in the case where a single band, say n, crosses the Fermi surface (which is necessary for realizing a topological superconducting state[24,25]), we can calculate the low-energy spectrum of the Hamiltonian from an effective Hamiltonian which is obtained by taking matrix elements of the BdG Hamiltonian in Eq. (1) with respect to the Nambu spinors

$$|n,\boldsymbol{k}\rangle_{\rm Nambu} = \begin{pmatrix} |n,\boldsymbol{k}\rangle \\ \Theta|n,-\boldsymbol{k}\rangle \end{pmatrix}, \qquad (3)$$

where $\Theta = i\sigma_y K$ with K being the complex conjugation operator. In this approximation, the translationally invariant part of the BdG Hamiltonian has the form

$$H_0(\boldsymbol{k},\boldsymbol{k}') = \begin{pmatrix} \epsilon_{\boldsymbol{k}} - \epsilon_{F,sm} & \Delta_{\boldsymbol{k}} \\ -\Delta^*_{-\boldsymbol{k}} & -(\epsilon_{-\boldsymbol{k}} - \epsilon_{F,sm}) \end{pmatrix} \delta(\boldsymbol{k}-\boldsymbol{k}'), \qquad (4)$$

where we have suppressed the band index n, since we are restricted to a single band and the term $H_{sm,\rm clean}(\boldsymbol{r}\sigma;\boldsymbol{r}'\sigma')$ has been replaced by its eigenvalue $\epsilon_{\boldsymbol{k}}$ in the relevant band. In the electron-doped case, $\epsilon_{\boldsymbol{k}}$ includes effects on the dispersion of the parameters V_Z and α [see Eq. (21)] while in the hole-doped case, it additionally contains information about the Luttinger parameters [see Eq. (29)]. We note that, in spite of its apparent complexity involving the superconducting proximity effect, spin-orbit coupling, Zeeman splitting, and disorder, we are still dealing here with an effective exactly solvable one-particle quantum problem.

For weak superconducting pairing and disorder scattering, the TS quasiparticle gap is determined by the energies and wave functions near the Fermi energy $\epsilon_{F,sm}$. In particular, we will approximate the dispersion around the Fermi energy by $\epsilon_{\boldsymbol{k}} \approx \epsilon_{F,sm} + v_F(|\boldsymbol{k}| - k_F)$, where v_F is the Fermi velocity. Moreover, since the relevant states are near the Fermi wave vector (i.e., $|\boldsymbol{k}| \approx k_F$), we will assume that matrix elements such as $\langle \boldsymbol{k}|\boldsymbol{k}_1\rangle$ depend only on the directions of the momenta $\boldsymbol{k}$ and $\boldsymbol{k}_1$. To calculate the matrix elements of $|\boldsymbol{k}\rangle$, we will assume that the Bloch eigenstates have a simple decomposition as

$$\langle \boldsymbol{r};\sigma|\boldsymbol{k}\rangle \equiv u_{\boldsymbol{k}}(\boldsymbol{r};\sigma) = e^{i\boldsymbol{k}\cdot\boldsymbol{r}} u_{\boldsymbol{k}}(\sigma). \qquad (5)$$

This assumption is valid as long as all perturbations involve momentum transfers that are smaller than a Bloch vector. For electrons σ is simply the electron spin. When applied to holes σ would represent the 4-component pseudospin degree of freedom associated with the Luttinger model.[7]

In this paper we will consider both 1D and 2D systems, and these cases will turn out to be closely related. In the two-dimensional case, we will restrict ourselves to rotationally symmetric systems with circularly symmetric Fermi surfaces where $\boldsymbol{k} = (k_F\cos\theta_{\boldsymbol{k}}, k_F\sin\theta_{\boldsymbol{k}})$. Using the azimuthal symmetry of the Bloch Hamiltonian corresponding to $H_{sm,\rm clean}$, we can define a Hermitian matrix R_z, which generates z-axis rotations so that

$$||k|,\theta_{\boldsymbol{k}}\rangle = e^{i(R_z-\lambda)(\theta_{\boldsymbol{k}})}||k|,0\rangle, \qquad (6)$$

where λ is chosen so that $||k|,\theta_{\boldsymbol{k}}\rangle$ is a single-valued function of $\theta_{\boldsymbol{k}}$. Since Kramers' theorem requires R_z to have half-integer eigenvalues $\lambda = 1/2$. For one-dimensional systems, such as electron- or hole-doped semiconducting nanowires, we will

consider systems with inversion symmetric Fermi points $\pm k_F$. In this case, the relevant states at the Fermi level are $|\pm k_F\rangle$. The 2D systems with Rashba spin-orbit coupling will turn out to have results that are solely dependent on the wave functions only at $|k_F,\theta_{\boldsymbol{k}} = 0,\pi\rangle$, which are identical in form to the states $|\pm k_F\rangle$ relevant for the 1D case. Therefore, these two cases are closely related and for results such as the quasiparticle gap in Eqs. (17) and (18), we will only state the result for the 1D case and imply a similar result in 2D, which can be derived easily.

The superconducting pairing potential $\Delta_{\boldsymbol{k}}$ in the projected Hamiltonian in Eq. (4) is the matrix element of Δ_0 in Eq. (1) between states near the Fermi level, which is written as

$$\Delta_{\boldsymbol{k}} = \Delta_0 \langle \boldsymbol{k}|\Theta|-\boldsymbol{k}\rangle. \tag{7}$$

Using Eq. (6) in the rotationally symmetric 2D case, $\Delta_{\boldsymbol{k}}$ simplifies to

$$\begin{aligned}\Delta_{\boldsymbol{k}} &= \Delta_0 \langle \boldsymbol{k}|\Theta|-\boldsymbol{k}\rangle = \Delta_0 \langle 0|e^{-i(R_z-\lambda)\theta_{\boldsymbol{k}}}\Theta e^{i(R_z-\lambda)\theta_{\boldsymbol{k}}}|\pi\rangle \\ &= e^{2i\lambda\theta_{\boldsymbol{k}}}\Delta_0\langle 0|\Theta|\pi\rangle = \Delta_0\langle 0|\Theta|\pi\rangle e^{i\theta_{\boldsymbol{k}}},\end{aligned} \tag{8}$$

where $\theta_{\boldsymbol{k}}$ is the angle of the wave vector $\boldsymbol{k}$ in the k_x-k_y plane. Here we have assumed that R_z, which transforms $k_F \rightarrow -k_F$, is odd under time-reversal symmetry. The TS quasiparticle gap for the Hamiltonian Eq. (4), in the absence of disorder [i.e., $V(\boldsymbol{r}) = 0$], is given by

$$\Delta = |\Delta_{\boldsymbol{k}}|. \tag{9}$$

The disorder scattering, induced by the potential $V(\boldsymbol{r})$ in Eq. (2), can be projected into states near the Fermi energy in a similar way as

$$V(\boldsymbol{k},\boldsymbol{k}') = \begin{pmatrix} v(\boldsymbol{k},\boldsymbol{k}') & 0 \\ 0 & -v^*(-\boldsymbol{k},-\boldsymbol{k}')\end{pmatrix}, \tag{10}$$

where $v(\boldsymbol{k},\boldsymbol{k}') = \langle \boldsymbol{k}|V(\boldsymbol{r})|\boldsymbol{k}'\rangle$. For spatially uncorrelated white noise disorder [i.e., $\langle V(\boldsymbol{r})V(\boldsymbol{r}')\rangle = v^2\delta(\boldsymbol{r}-\boldsymbol{r}')$], and using the simple form for the Bloch functions Eq. (5), the disorder propagator $\langle v(\boldsymbol{k}_1,\boldsymbol{k}_2)v(\boldsymbol{v}_3,\boldsymbol{k}_4)\rangle$ can be written as

$$\langle v(\boldsymbol{k}_1,\boldsymbol{k}_2)v(\boldsymbol{v}_3,\boldsymbol{k}_4)\rangle = v^2\langle \boldsymbol{k}_1|\boldsymbol{k}_2\rangle\langle \boldsymbol{k}_3|\boldsymbol{k}_4\rangle. \tag{11}$$

The disorder strength v^2 is related to the mean-scattering time (i.e., momentum relaxation time)

$$\tau_{sm} = \frac{1}{\pi v^2 N(0)}, \tag{12}$$

which in turn can be determined experimentally from mobility measurements using the equation

$$\mu_{sm} \approx \frac{e\tau_{sm}}{m^*}, \tag{13}$$

where m^* is the transport effective mass and $N(0)$ is the density of states at the Fermi surface. Note that we have dropped a matrix-element factor in determining the scattering time in Eq. (12). This is partly to account for multiband effects that we are not directly accounting for in this paper. Since we are using mobility only as a qualitative estimator of the scattering, the combination of Eqs. (12) and (13) provide a good estimate of the disorder scattering v^2. Although Eqs. (12) and (13) strictly apply only in the case of white noise disorder arising from short-ranged impurity scattering, we assume that they remain valid for long-range disorder as well in the presence of random charged impurity scattering since carrier screening of the impurity potential should render the Coulomb disorder into an effective short-range disorder. In addition, our use of τ_{sm} to operationally characterize the semiconductor disorder should be qualitatively valid for any kind of impurity potential. While we have made a single Fermi surface approximation in Eq. (4), this is more for the sake of simplicity. In the next paragraph, we will comment on how our results generalize to the multiple Fermi surface case, as for example in the case of multiband occupancy in the semiconductor nanowire where the Fermi level could lie in some high subband rather than the ground 1D subband.[17]

The topological superconducting quasiparticle gap in the presence of a disorder potential may be determined by calculating the disorder-averaged Green's function within the Born approximation.[26] The disorder-averaged Green's function can be calculated from the self-energy Σ using the Dyson equation

$$G^{-1}(\boldsymbol{k},\omega) = G_0^{-1}(\boldsymbol{k},\omega) - \Sigma(\boldsymbol{k},\omega), \tag{14}$$

where the Green's function for the clean system is given by

$$\begin{aligned}G_0^{-1}(\boldsymbol{k},\omega) &= [\omega - H_0(\boldsymbol{k})] \\ &= \omega - (\epsilon_{\boldsymbol{k}} - \epsilon_{F,sm})\tau_z - \Delta_{\boldsymbol{k}}\tau_+ - \Delta_{\boldsymbol{k}}^*\tau_-.\end{aligned} \tag{15}$$

The self-energy $\Sigma(\boldsymbol{k},\omega)$ is approximated within the self-consistent Born approximation[26] as

$$\Sigma_{\alpha\beta}(\boldsymbol{k},\boldsymbol{k}') = \int d\boldsymbol{k}_1 \langle V_{\alpha\lambda}(\boldsymbol{k},\boldsymbol{k}_1)V_{\delta\beta}(\boldsymbol{k}_1,\boldsymbol{k})\rangle G_{\lambda\delta}(\boldsymbol{k}_1)\delta(\boldsymbol{k}-\boldsymbol{k}'), \tag{16}$$

where $\langle V_{\alpha\lambda}(\boldsymbol{k},\boldsymbol{k}_1)V_{\delta\beta}(\boldsymbol{k}_1,\boldsymbol{k})\rangle$ is the disorder propagator from Eqs. (10) and (11), $\alpha,\beta,\lambda,\delta$ are Nambu indices, and for brevity of notation we have dropped the ω dependence of Σ and G in this equation. The self-energy within the first-order Born approximation is obtained by replacing G by G_0 in Eq. (16). The disorder calculation for the case of multiple Fermi-surfaces follows in an analogous way. Since momentum is a good quantum number in Eq. (14), Eq. (14) does not couple the multiple Fermi surfaces and therefore can be solved for each Fermi surface separately. The self-energy term Eq. (16) in principle has contributions from all Fermi surfaces. However, it is dominated by the contribution from the Fermi surface with the smallest gap. Therefore, our calculation, which focuses on the Fermi surface with the smallest gap, is expected to yield qualitatively correct results.

Solving the Dyson equations in the first-order Born approximation in the 1D and 2D cases, as discussed in Appendix A, we obtain the disorder-averaged TS quasiparticle gap

$$E_g = \Delta\left[1 - \frac{1}{2^{1/3}}(\pi\tau_{sm}\Delta)^{-2/3}|\langle k_F| -k_F\rangle|^{4/3}\right]. \tag{17}$$

Note that the disorder renormalization of the gap vanishes in the time-reversal symmetric limit since in that case $|\boldsymbol{k}\rangle$ and $|-\boldsymbol{k}\rangle$ are Kramers pairs and $\langle k_F| -k_F\rangle = 0$. The result Eq. (17) gives the reduction in the quasiparticle gap due to weak disorder within the first-order Born approximation.

The Dyson equations, Eqs. (14) and (16), can in fact be solved for arbitrary disorder strengths within the self-consistent Born approximation as explained in Appendix B.

The resulting TS state quasiparticle gap in the presence of disorder is found to be

$$E_g = \Delta\sqrt{1 - 3x + 3x^2 - 3x^3}, \tag{18}$$

where $x = (\pi\tau_{sm}\Delta)^{-2/3}|\langle k_F| - k_F\rangle|^{4/3}$. Note that the gap E_g within the first-order Born approximation in Eq. (17) is not simply obtained by taking the limit of small x in the self-consistent Born result Eq. (18). This is because the Born approximation is a series expansion in terms of the Green's function, which has a pole at $\omega \sim E_g$, so that the expansion parameter in the series expansion diverges (at any value of x) at the relevant point and one cannot expect the lowest order approximation to match the self-consistent result. Despite this technical point, the first-order and self-consistent Born approximation results, Eqs. (17) and (18), are qualitatively similar at small values of the parameter x.

The above equation is valid as long as the expression under the square root is positive. In fact, the quasiparticle gap E_g closes for sufficiently strong disorder (or sufficiently small $\Delta\tau_{sm}$) so that, by solving for $E_g = 0$ in Eq. (18), the disorder scattering time is found to satisfy the lower bound

$$\tau_{sm} > \frac{3.4}{\pi}\hbar\Delta^{-1}|\langle k_F| - k_F\rangle|^2, \tag{19}$$

above which the TS state quasiparticle gap $E_g > 0$. In this paper, we will also assume that $\tau_{sm} > 1/\tilde{\epsilon}_{F,sm}$ ($\tilde{\epsilon}_{F,sm}$ is the Fermi energy with respect to the bottom of the topmost filled band) need not be strictly enforced because of the existence of multiple bands in the actual experimental system, which will evade the localization problem.

From Eqs. (13) and (19), we find that the TS state gap induced on the Fermi surface survives as long as the mobility of the system exceeds the threshold

$$\mu_{sm} > 3.4\frac{e\hbar}{\pi m^*\Delta}|\langle k_F| - k_F\rangle|^2. \tag{20}$$

This suggests that the mobility threshold can be decreased by decreasing the Kramers pair overlap $|\langle k_F| - k_F\rangle|$, which, as we show in Eq. (27), can be achieved by reducing the Zeeman potential. We will apply all these results to electron- and hole-doped semiconductors in the following two sections.

III. PROXIMITY-COUPLED ELECTRON- AND HOLE-DOPED SEMICONDUCTORS

In this section we review the two recently proposed systems, electron- and hole-doped semiconductors, to which we will apply our results derived in the previous section.

A. Electron-doped semiconductors

For 2D electron-doped semiconductors with Rashba and Zeeman couplings, $H_{sm,\text{clean}}$ in Eq. (2) can be written as

$$H_{sm,\text{clean}}(k) = \frac{k^2}{2m^*} + \alpha(\boldsymbol{k}\times\boldsymbol{\sigma})\cdot\hat{\boldsymbol{z}} + V_Z\sigma_y - \epsilon_{F,sm}, \tag{21}$$

where m^* is the effective mass of the electrons, α is the Rashba spin-orbit coupling constant, and V_Z is the Zeeman splitting. For a one-dimensional nanowire along the y axis, the above Hamiltonian reduces to

$$H_{sm,\text{clean}}(k) = \frac{k^2}{2m^*} + \alpha k\sigma_x + V_Z\sigma_y - \epsilon_{F,sm}. \tag{22}$$

For a chemical potential $|\epsilon_{F,sm}| < V_Z$, the above Rashba spin-orbit-coupled Hamiltonian has a single band at the Fermi level with an eigenstate described by the spinor

$$|k_F\rangle = \frac{1}{\sqrt{2\left[V_Z^2 + \alpha^2k_F^2 + V_Z\sqrt{V_Z^2 + \alpha^2k_F^2}\right]}} \times \begin{pmatrix} \alpha k_F \\ -\sqrt{V_Z^2 + \alpha^2k_F^2} - V_Z \end{pmatrix}. \tag{23}$$

Now, using Eq. (9), the superconducting quasiparticle gap in the clean electron-doped case is given by

$$\Delta \sim \frac{\alpha k_F}{\sqrt{V_Z^2 + \alpha^2k_F^2}}\Delta_0. \tag{24}$$

The proximity-induced pairing potential in the semiconductor, Δ_0, can be related to the pairing potential in the bulk superconductor Δ_s by the relation[27]

$$\Delta_0 = \Delta_s\frac{\lambda}{\lambda + \Delta_s}, \tag{25}$$

where

$$\lambda = \pi|t|^2\rho_{SC}(E_F). \tag{26}$$

Here t represents the tunneling matrix element between the semiconductor and the superconductor, $\rho_{SC}(E_F)$ is the normal state density of states of the superconductor, and λ gives the rate at which electrons from the semiconductor tunnel into the superconductor.[27] We note that for weak tunneling $\Delta_0 \sim \lambda$, and for strong tunneling $\Delta_0 \sim \Delta_s$. The superconducting proximity effect in electron-doped InAs/superconducting Al interfaces has been already been observed to lead to $\Delta_0 \sim \Delta_s \sim 2$ K,[28] so that one can infer that the transparency parameter $\lambda \gtrsim \Delta_s$. The Kramer-pair overlap $\langle k_F| - k_F\rangle$, which determines the effect of disorder scattering via Eq. (18), is then given by

$$\langle k_F| - k_F\rangle = \frac{V_Z}{\sqrt{V_Z^2 + \alpha^2k_F^2}}, \tag{27}$$

which in the limit $V_Z/\alpha k_F \ll 1$ becomes $\langle k_F| - k_F\rangle \sim V_Z/\alpha k_F$.

B. Hole-doped semiconductors

Recently, it has also been proposed[7] that hole-doped nanowires, because of the possibly stronger spin-orbit coupling[22,23] and larger effective mass of holes, might be a better candidate for creating topological superconductors and Majorana fermions. The hole bands of a group III-V semiconductor such as InAs or GaAs are composed of p orbitals, which have orbital angular momentum $L = 1$. Because of strong spin-orbit coupling and cubic symmetry of these semiconductors, the description of the states near the top of the valence band at $\boldsymbol{k} = 0$ must be written in terms of

spin-3/2 total angular momentum matrices $\boldsymbol{J} = \boldsymbol{L} + \boldsymbol{S}$. The total spin-1/2 manifold of states forms a split-off band, which is separated by a large energy and therefore can be ignored. The resulting three-dimensional Hamiltonian is known as the four-band Luttinger model,[29] which is written as

$$H_{3D} = \frac{1}{2m_0}\left[\left(\lambda_1 + \frac{5}{4}\lambda_2\right)p^2 - 2\lambda_2 \sum_{\alpha=x,y,z} p_\alpha^2 J_\alpha^2\right] - \lambda_3 \frac{1}{2m_0} \sum_{\alpha\neq\beta=x,y,z} p_\alpha p_\beta J_\alpha J_\beta, \quad (28)$$

where $\boldsymbol{p} = -i\nabla$ and $\gamma_{1,2,3}$ are effective Luttinger parameters. The effective mass m_0 for the holes is negative so that the curvature of the valence bands are inverted with respect to the conduction bands. We will consider a nanowire formed by confining the bulk hole-doped semiconductor confined strongly along the x and z directions, so that the confinement energy scale $\sim 1/2m_0L_y^2$ is large compared to all energy scales we will be interested in. Therefore one can project the three-dimensional Hamiltonian H_{3D} into the lowest confinement band of the nanowire by replacing $p_{x,z} \to \langle p_{x,z}\rangle = 0$, $p_{x,z}^2 \to \langle p_{x,z}^2\rangle = \pi^2/L_z^2$ and adding a Rashba spin-orbit coupling proportional to α[23,31,32] and a Zeeman term proportional to V_Z to account for electric-field-induced inversion symmetry breaking and magnetic-field-induced time-reversal symmetry breaking, respectively. The resulting Hamiltonian for a hole-doped nanowire along y with a Rashba coupling (for the lengths in the transverse directions $L_z = L_x$) is given by[7]

$$H_{sm,\text{clean}}(k) = -\left(\frac{\lambda_1}{2} + \frac{5\lambda_2}{4} - \lambda_2 J_y^2\right)k^2 - \alpha k J_x + \frac{2\beta_2}{\sqrt{3}}\left(\frac{15}{4} - J_y^2\right) + V_Z J_y - \epsilon_{F,sm}, \quad (29)$$

where $\beta_2 = \pi^2\lambda_2\sqrt{3}/2L_z^2$. The Hamiltonian at $k = 0$ commutes with J_y^2. Moreover, the states with $J_y^2 = 1/4$ form the highest energy states in the valence band. These states also have the lower effective mass of the two manifolds $J_y^2 = 1/4, 9/4$ of states. Note that this is opposite to the two-dimensional case, where the heavy hole is closer to the band edge. Thus the light-hole states with $J_y = \pm 1/2$ form the set of states closest to the band edge and we can restrict to this two-dimensional subspace $J_y = \pm 1/2$, where we identify $J_y = \sigma_y = \pm 1/2$ as a pseudospin variable. In this subspace, $J_x \sim \sigma_x$ and $J_z \sim \sigma_z$, so that the Hamiltonian for the two upper bands effectively becomes

$$H_{sm,\text{clean}}(k) = -\left(\frac{\lambda_1}{2} + \lambda_2\right)k^2 - \alpha k\sigma_x + V_Z\sigma_y + \epsilon_{F,sm}. \quad (30)$$

The hole Hamiltonian Eq. (30), in the specific isotropic limit we consider, is identical (up to sign) to the one-dimensional electron-doped Rashba Hamiltonian in Eq. (22) and therefore one can expect most of the physics discussed in the previous subsection for the electron-doped nanowire in this limit to translate to the hole-doped case, except for the different effective mass and Rashba spin-orbit coupling. While the band structure of the hole-doped wire is quite similar to the electron-doped case, it is not obvious from this discussion that the s-wave proximity effect has the same form in the σ spin space. In principle, the proximity-induced effective superconducting pairing potential Δ_0 at an interface between the semiconductor and the superconductor can be calculated by projecting the anomalous self-energy Σ_{SC} induced by proximity to the superconductor,[27] into the low-energy space of states $|\sigma_y = \pm 1/2\rangle$. Since these states form a Kramers pair, one can see that time-reversal symmetry only allows a conventional spin-singlet pairing in the $\sigma_y = \pm 1/2$ space. Furthermore, the subspace of states in the $|\sigma_y = \pm 1/2\rangle$ basis may be expanded in terms of the original spin eigenstates $|m_S = \pm\frac{1}{2}\rangle$ and $|L_{x,y,z} = 0\rangle$ (which are related to the orbital angular momentum eigenstates $|m_L = 0, \pm 1\rangle$ by a unitary transformation) as

$$\left|\sigma_y = +\frac{1}{2}\right\rangle \equiv \left|J_y = \frac{1}{2}\right\rangle = \frac{1}{\sqrt{3}}\left[\left|L_x = 0, S_y = -\frac{1}{2}\right\rangle + i\left|L_z = 0, S_y = -\frac{1}{2}\right\rangle - \left|L_y = 0, S_y = \frac{1}{2}\right\rangle\right], \quad (31)$$

$$\left|\sigma_y = -\frac{1}{2}\right\rangle \equiv \left|J_y = -\frac{1}{2}\right\rangle = \frac{1}{\sqrt{3}}\left[\left|L_x = 0, S_y = \frac{1}{2}\right\rangle - i\left|L_z = 0, S_y = \frac{1}{2}\right\rangle - \left|L_y = 0, S_y = -\frac{1}{2}\right\rangle\right]. \quad (32)$$

To calculate Δ_0, which is related to the matrix element $\langle\sigma_y = +1|\Sigma_{SC}|\sigma_y = -1\rangle$ of a spatially smoothly varying (on the orbital scale) proximity-induced self-energy Σ_{SC}, one can ignore the matrix elements involving the orbital $|L_x = 0\rangle, |L_z = 0\rangle$ for SC interfaces normal to the $\hat{z}$ axis. This leads to the effective barrier transparency parameter λ in Eq. (25) to be reduced by a factor of 3. The corresponding pairing potential Δ_0 from Eq. (25) is not significantly affected and remains the same between electrons and holes provided a moderately transparent barrier with $\lambda > \Delta_s$ can be achieved. Therefore, more generally, one can expect a proximity effect where the transparency factor of the Sm/SC interface, λ, is suppressed by at most a factor of order 1, with a value for the pairing potential $\Delta_0 \sim \Delta_s$, even for holes.

To summarize, while the hole-doped nanowires have fundamentally different microscopic Hamiltonians consisting of a triplet of orbitals with p symmetry, for nanowires it is possible to work in the limit of symmetric confinement along the two directions transverse to the wire, where we have shown that the effective Hamiltonian and proximity effect are identical in form to the electron-doped wire case. Of course, the parameters in the Hamiltonian are expected to be quite different and in particular the effective mass and Rashba spin-orbit coupling are expected to be much larger.[22,23] At the same time, the corresponding mobility for the semiconductors that can be achieved are found to be significantly lower,[36] indicating much stronger disorder for hole-doped systems. Thus, the hole systems have the advantage (disadvantage) of stronger SO coupling (larger disorder), and whether the net prospect for realizing the non-Abelian Majorana mode is greater in hole-based systems (than in the electron-based systems) or not will depend entirely on which of these

two effects wins over in realistic samples. Another possible advantage of the hole systems is the higher value of the Landé g factor which necessitates weaker magnetic field values in achieving the condition for topological superconductivity. One should, however, realize that very little actual experimental work exists in hole-based semiconductor nanowires. However, it is encouraging that the superconducting proximity effects in both electron- and hole-based semiconductors have been observed in experiments.[28,30] Therefore, we do believe that the hole-based systems (e.g., InAs, InSb, SiGe, and perhaps even GaAs) should be included in the experimental search for the Majorana mode in semiconductor-superconductor heterostructures.

IV. TS STATE QUASIPARTICLE GAP IN THE PRESENCE OF DISORDER

The clean-limit quasiparticle gap Δ in the topological superconducting state can be obtained for the Rashba spin-orbit-coupled Hamiltonian Eq. (21) using Eqs. (24) and (25) as

$$\Delta = \frac{\lambda\Delta_s}{\lambda+\Delta_s}\frac{\alpha k_F}{\sqrt{V_Z^2+\alpha^2k_F^2}}. \tag{33}$$

This expression suggests that to obtain a large gap, Δ, in the semiconductor one should restrict oneself to the limit where $\alpha k_F \gtrsim V_Z$. Moreover, to remain in the requisite odd subband (confinement bands) limit it is also necessary to choose a chemical potential $\epsilon_{F,sm}$ in the gap (at $\boldsymbol{k}=0$) induced by the Zeeman splitting V_Z.[3] This restricts $k_F \approx \frac{m^*\alpha}{2}$ in the highest filled subband. In this limit one can approximate $\alpha k_F \approx E_{\rm SO} = 2m^*\alpha^2$, which we call the spin-orbit energy $E_{\rm SO}$. This spin-orbit energy $E_{\rm SO}$ is a crucial energy scale in the problem which is to be compared with the other independent energy scales such as V_Z, Δ_s, and $1/\tau_{sm}$. Therefore, from Eq. (30), to obtain a large quasiparticle gap at the Fermi surface the system must be restricted to the regime

$$V_Z \lesssim E_{S0}. \tag{34}$$

The semiconductor system is in the topological state if and only if the Pfaffian invariant of the relevant BdG Hamiltonian is negative,[33] which is equivalent to the topological condition

$$\tilde{V}_Z^2 > \tilde{\Delta}_0^2 + \tilde{\epsilon}_{F,sm}^2, \tag{35}$$

where $\tilde{V}_Z = V_Z/(1+\lambda/\Delta_s)$, $\tilde{\Delta}_0 = \Delta_0$, and $\tilde{\epsilon}_{F,sm} = \epsilon_{F,sm}/(1+\lambda/\Delta_s)$ are the renormalized parameters in the effective Hamiltonian of the proximity-coupled semiconductor after the superconductor has been integrated out.[3,27] Thus, using Eqs. (25) and (35), the topological condition in terms of the bare parameters can be written as

$$V_Z^2 > \lambda^2 + \epsilon_{F,sm}^2. \tag{36}$$

Equations (36) and (34), together with Eq. (18) [or Eq. (20)], define the optimal constraints on the material considerations for the realization of the TS phase in the semiconductor.

In what follows, we assume that the system is reasonably deep in the topological superconducting phase (i.e., $V_Z > 2\lambda, 2\epsilon_{F,sm}$) so the smallest gap occurs near the Fermi wave vector $|\boldsymbol{k}| \sim k_F$ instead of near $|\boldsymbol{k}| \sim 0$.[3] Therefore in attempting to optimize the quasiparticle gap one notices from Eqs. (34) and (36) a hierarchy of energy scales

$$E_{\rm SO} > V_Z > 2\lambda > 2\Delta > 2E_g. \tag{37}$$

The first two inequalities from the left are constraints between the external parameters $E_{\rm SO}, V_Z$, and λ, out of which V_Z and λ must be tuned to satisfy the above inequality. The other external parameter is the disorder scattering rate in the semiconductor, τ_{sm}^{-1}, which must be reduced to satisfy $\Delta > (\pi\tau_{sm})^{-1}\sqrt{1+E_{\rm SO}^2/V_Z^2}$. The two inequalities on the right-hand side of Eq. (37) are between the derived quantities Δ and E_g, which are completely determined once $E_{\rm SO}, V_Z, \lambda, \tau_{sm}$ are given, so that the conditions $2\lambda > 2\Delta$ and $2\Delta > 2E_g$ follow as direct consequences of Eqs. (33) and (18), respectively. Therefore, the disordered TS state quasiparticle gap, E_g, is constrained by the spin-orbit energy scale $E_{\rm SO}$, which must be as large as possible in the problem.

In the presence of disorder, one can use Eq. (18) together with Eq. (27) to show that for $V_Z \lesssim E_{\rm SO}$, the disorder-renormalized TS state quasiparticle gap is given by

$$E_g = \Delta\sqrt{1-3x+3x^2-3x^3}, \tag{38}$$

where $x = (\pi\tau_{sm}\Delta)^{-2/3}(V_Z/\sqrt{V_Z^2+E_{\rm SO}^2})^{4/3}$. The mobility threshold, which is the minimum mobility required to realize a nonzero TS state gap E_g in the presence of disorder, is obtained by using Eqs. (20) and (27) to be

$$\mu_{sm} > 6.8\frac{e\hbar V_Z(\Delta_s+V_Z/2)}{\pi m^*\Delta_s E_{\rm SO}\sqrt{V_Z^2+E_{\rm SO}^2}}, \tag{39}$$

which vanishes in the limit $V_Z \to 0$. Note that we have reintroduced the $\hbar = 1$ to make the expression dimensionally consistent. Since μ_{sm} increases with Δ, which in turn increases with λ, for deriving Eq. (39), we have assumed the λ is chosen to reach its maximum value $\lambda = V_Z/2$, above which the system can no longer be considered to be deep in the topological phase [see Eq. (37)]. In fact, we will assume that V_Z has been tuned to be $V_Z = 2\lambda$ for the rest of the paper.

Of course, from Eq. (36), there is a threshold value for V_Z only above which the TS state itself is realized. Therefore, V_Z cannot be taken as zero in Eq. (38) to maximize the disordered TS state gap E_g. In Eq. (38), to deduce the optimum E_g, we use the right-hand side of Eq. (33) to substitute for Δ and, for a robust topological state, we take $\lambda = V_Z/2$. The right-hand side of Eq. (38) is then a function of V_Z, τ_{sm} (or $\mu_{sm} \sim e\tau_{sm}/m^*$), Δ_s, and $E_{\rm SO}$. Among these Δ_s (the gap in the adjacent superconductor) and $E_{\rm SO}$ (the spin-orbit coupling energy in the semiconductor) are known experimental quantities. Therefore Eq. (38) defines a formula for E_g in terms of V_Z parametrically related by μ_{sm}. For given values of μ_{sm}, we maximize E_g with respect to V_Z and plot these maximized values of E_g as a function of μ_{sm} for electron- and hole-doped semiconductors in Figs. 1 and 2, respectively. These plots are the central results of this paper.

From Fig. 1 it is clear that for electron-doped wires with a mobility of 100 000 cm^2/V-s,[35] which has been achieved for wires with a diameter 60 nm, a measurable robust TS state gap of 50–100 mK is achievable. As is also clear from Fig. 2, for hole-doped wires with a significantly larger

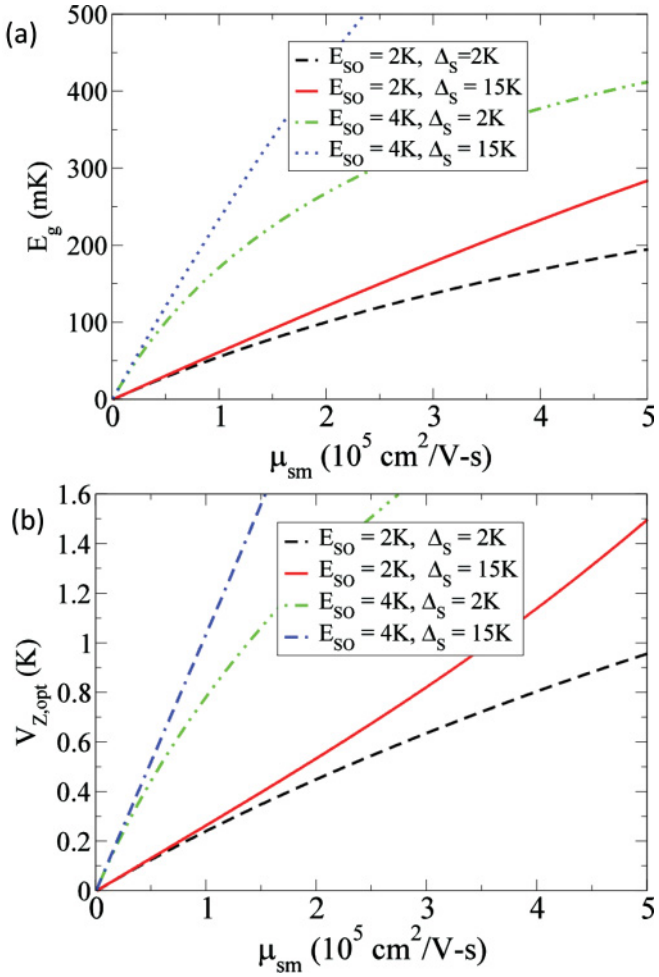

FIG. 1. (Color online) (a) Calculated disordered TS state quasiparticle gap E_g as a function of semiconductor mobility μ_{sm} for electron-doped wires with $E_{SO} = 2m^*\alpha^2 = 2$ K (Ref. 34) and $E_{SO} = 4$ K allowing for future electric-field-enhanced spin-orbit coupling (Ref. 37). (b) The values of $V_Z = 2\lambda$ realizing E_g in panel (a) plotted with μ_{sm}. The gaps in the adjacent bulk superconductor are taken to be $\Delta_s = 2$ K corresponding to Al and $\Delta_s = 4$ K corresponding to Nb.

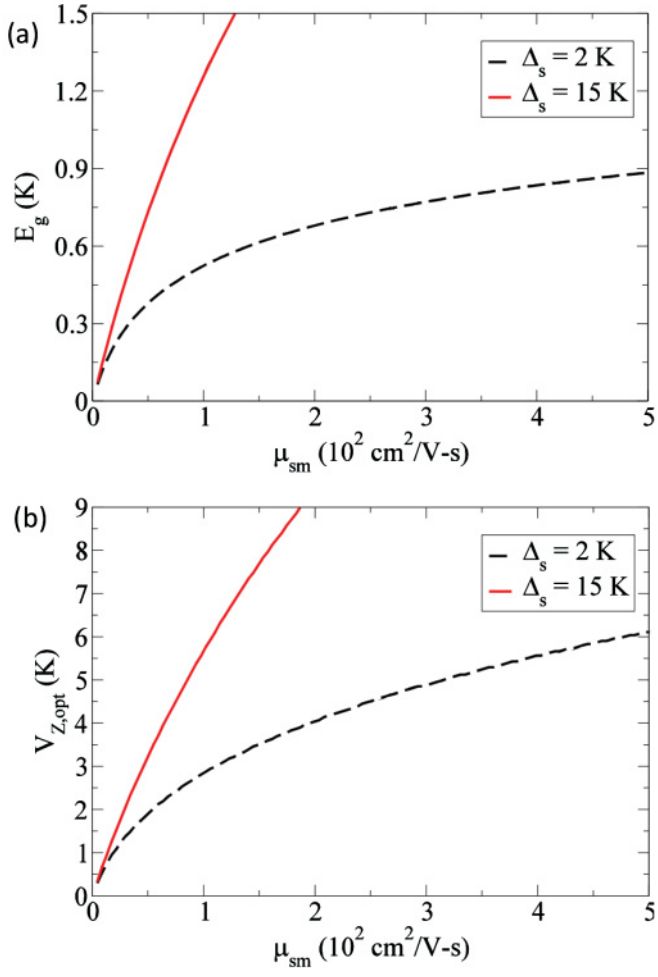

FIG. 2. (Color online) (a) Calculated disordered TS state quasiparticle gap E_g as a function of semiconductor mobility μ_{sm} for hole-doped wires with $E_{SO} = 300$ K (Refs. 22 and 23). (b) The values of $V_Z = 2\lambda$ realizing E_g in panel (a) plotted with μ_{sm}. The gaps in the adjacent bulk superconductor are taken to be $\Delta_s = 2$ K corresponding to Al and $\Delta_s = 4$ K corresponding to Nb.

spin-orbit energy $E_{SO} \sim 30$ meV, a larger gap of 0.8 K is achievable for a mobility of 100 cm^2/V-s.[36] It should be noted that in general the holes have much lower mobilities than electrons in the same semiconductor material even after taking into account their large effective mass difference.

V. SUMMARY AND CONCLUSION

In this paper we have addressed the effects of disorder from the semiconductor surface on the stability of the topological superconducting state on 1D and 2D electron- and hole-doped semiconductors proximity coupled to bulk 3D s-wave superconductors. In recent works[17] it has been shown that the effects of disorder from the adjacent bulk superconductor on the TS state is minimal, so we have ignored this effect. However, since the TS state in the semiconductor explicitly breaks the time-reversal symmetry (due to an external Zeeman splitting), even the disorder from the semiconductor surface itself has an effect on the stability of the TS state and will close the BCS-like superconducting quasiparticle gap at the semiconductor Fermi surface for low enough mobility. We have shown that the disordered TS state quasiparticle gap E_g is suppressed with increasing values of the ratio r between the Zeeman splitting V_Z and the spin-orbit energy scale $E_{SO} = 2m^*\alpha^2, r = V_Z/E_{SO}$. The dimensionless quantity r measures the extent of the TR symmetry breaking in the semiconductor to produce the TS state and Majorana fermions.

Our main results are plotted in Figs. 1 and 2. They display the achievable disorder-renormalized TS state gap E_g as a function of the semiconductor mobility μ_{sm} in both electron- and hole-doped semiconductor wires. From Fig. 1 we find that for electron-doped wires with a mobility of 100 000 cm^2/V-s,[35] which has been achieved for wires with a diameter 60 nm, a measurable robust TS state gap of 50–100 mK is achievable.

From Fig. 2 we find that for hole-doped wires with a significantly larger spin-orbit energy $E_{\rm SO} \sim 30$ meV, a larger gap of 0.8 K is achievable for a mobility of 100 cm^2/V-s.[36] Thus, despite the fact that the semiconductor TS state breaks the time-reversal symmetry, realizing a robust TS state is possible in both electron- and hole-doped systems even in the presence of realistic disorder on the surface of the semiconductor.

Before concluding, it may be useful to provide a qualitative discussion and a general perspective on the issue of optimal materials for the realization of the predicted TS phase and Majorana modes in semiconductor-superconductor sandwich structures. The first point to emphasize is that there are far too many independent physical parameters entering the problem for theory to be particularly useful in this context. At least six independent material parameters play a role here: α, k_F, V_Z, $\epsilon_{F,sm}$, Δ_s, t [which determines λ in Eq. (26)]. In addition, disorder, which plays a crucial role by the nonexistence of Anderson's theorem in the time-reversal invariance broken (i.e., $V_Z \neq 0$) situation, is itself characterized by several independent physical mechanisms: disorder in the adjacent bulk superconductor, long-ranged disorder in the semiconductor, disorder-induced fluctuations in t, interface disorder, puddles, and so on. A physical system characterized by such a large (>10) set of independent parameters, all of which are important in determining the fate of the TS state, is not an easy optimization problem to deal with theoretically. In particular, it may turn out to be more practical to simply carry out experiments on available systems (e.g., InAs or InSb on Al or Nb) than to trust precise theoretical quantitative predictions with respect to the optimal materials choice.

With these important caveats in mind, we can, nonetheless, make some general qualitative statements, quite apart from the more precise quantitative statements made in the main body of this work. In the clean case, where disorder is not an issue (i.e., extreme high-mobility semiconductor systems), it is obvious that the semiconductor spin-orbit coupling should be as large as possible. This continues to be the case even in the presence of disorder, making $E_{\rm SO}(\approx \alpha k_F)$ to be the key physical parameter, which should be made as large as possible (including enhancement by external gates if feasible[37]) with no constraints. Similarly, disorder is always harmful to the TS state, and therefore $1/\tau_{sm}$ should be made as small as possible by working with the highest mobility materials. Although having a spin-orbit coupling strength as large as possible is obviously helpful to the realization of the TS phase, this may have the detrimental effect of enhancing impurity-induced scattering between the spin-split bands, thus reducing the mobility,[38] and therefore some optimization may be necessary even with respect to spin-orbit coupling and mobility in order to satisfy the general requirement of having both the highest possible spin-orbit coupling and mobility.

The same is to a limited degree true of the superconducting gap Δ_s (or equivalently T_c) in the bulk supercnoductor, but this advantage is considerably nullified by the fact that the proximity effect is determined primarily by the parameter λ [see Eq. (25)], and this parameter should be made as large as possible, even at the cost of having a lower Δ_s in the bulk superconductor (e.g., Al may be preferable over Nb if $\lambda_{\rm Al} > \lambda_{\rm Nb}$). We note that having an arbitrarily large proximity gap Δ_0 in the semiconductor may not necessarily help unless $E_{\rm SO}$ can also be simultaneously increased (e.g., by an external gate) since $E_{\rm SO} > V_Z > 2\lambda > 2\Delta > 2E_g$ is a necessary condition for the existence of the TS phase. Similarly, having a very small V_Z does not help since $V_Z > 2\Delta$ determines the condition for a robust topological phase, and having a small V_Z necessarily requires having a much smaller Δ, which severely restricts the temperature range where the experiments investigating the topological phase can occur since $T < \Delta$ is necessary. For the same reason a small $E_{\rm SO}$, e.g., GaAs, with correspondingly smaller V_Z and Δ would not work either since the operational temperature would then be too small.

As for disorder, our discussion in this work has considered the semiconductor disorder to be short ranged, which is consistent with interface disorder (or roughness) scattering which is known to be important in semiconductor nanowires. Carrier screening should render long-range Coulomb disorder arising from random charged impurities in the semiconductor into effective short-ranged disorder, making our model of rather general validity. The fact that we model disorder through an effective relaxation time τ_{sm} defined through the measured carrier mobility makes the model robust with respect to different types of disorder in the semiconductor, but we note that for long-ranged Coulomb disorder τ_{sm}^{-1} is really only a lower bound on the effective disorder. (Disorder arising from impurities in the superconductor does not affect the TS phase at all; see Ref. 17 for details.)

A simple dimensional argument, which has been authenticated by a renormalization group calculation,[39] suggests $\Delta\tau_{sm} > 1$, i.e., $\tau_{sm}^{-1} < \Delta$, as the bound on the effective scattering rate for the topological gap Δ to survive disorder in a spinless chiral p-wave superconductor characterized only by these two parameters (unlike our problem which is characterized by many physical parameters). We note that our microscopic Born approximation calculation [Eq. (19)] is consistent with this case deep in the TS phase for $V_Z \sim E_{\rm SO}$. For $E_{\rm SO} \gg V_Z$, the effect of disorder scattering is suppressed so that the topological gap survives disorder for a broader range of parameters $\Delta\tau_{sm} > (V_Z/E_{\rm SO})^2$. Unfortunately for the semiconductor-superconductor sandwich structures of interest to us, $\Delta\tau_{sm} > (V_Z/E_{\rm SO})^2$ only provides a necessary condition since Δ cannot be made arbitrarily large unless $E_{\rm SO}$, i.e., the spin-orbit coupling, is itself arbitrarily large. The sufficient conditions for the gapped topological state to exist in the semiconductor sandwich structures are given by Eqs. (33) and (34), which require "large" V_Z making it necessary to have even larger $E_{\rm SO}$. Thus, the existence of the TS phase in the realistic semiconductor sandwich structures depends on the seamless and multiparameter materials optimization of spin-orbit coupling, spin splitting, superconducting gap, and disorder in an interdependent manner.

We conclude with the observation that the single most important ingredient for the TS state to emerge in semiconductor-superconductor sandwich structures is to have a large spin-orbit coupling and high mobility. For electrons both InAs and InSb satisfy the necessary requirements if the mobility can be enhanced around 10^5 cm^2/V-s. For holes the spin orbit coupling being very large, much lower mobilities ($\sim 10^2$ cm^2/V-s) should work. These considerations imply that holes should be looked into experimentally for the realization

of the TS phase. In addition, having several (odd number of) subbands[40] occupied in the nanowire should help since it reduces disorder through screening and enhances the effective values of E_{SO}. We emphasize that the existence of the TS state depends delicately on the competition among superconducting proximity effect, spin-orbit coupling, spin splitting, and chemical potential. (Disorder scattering always suppresses the TS state.) As such, any materials optimization must carefully choose among these physical parameters while at the same time maintaining the highest possible mobility (i.e., smallest possible disorder scattering). The experimental search for the Majorana mode should thus concentrate on semiconductor systems of the highest mobility and the strongest SO coupling using the appropriate superconductors which produce the best quality interface between the superconductor and the semiconductor.

ACKNOWLEDGMENTS

This work is supported by DARPA-MTO, DARPA-QuEST, JQI-NSF-PFC, Microsoft-Q, and NSF. We thank Chuanwei Zhang for helpful discussions.

APPENDIX A: DYSON EQUATIONS AND DISORDER-AVERAGED GREEN's FUNCTION

In this Appendix, we start by first simplifying the Dyson equations Eqs. (14) and (16) and then solve the equations for the first-order Born approximation case. The self-consistent Born approximation is solved in Appendix B. Substituting Eqs. (10) and (11) into Eq. (16), the self-energy Σ is written as

$$\begin{aligned}\Sigma(\boldsymbol{k}) = v^2 \int d\boldsymbol{k}_1 \Big[& |\langle \boldsymbol{k}|\boldsymbol{k}_1\rangle|^2 \frac{(1+\tau_z)}{2} G(\boldsymbol{k}_1) \frac{(1+\tau_z)}{2} \\ & + |\langle -\boldsymbol{k}|-\boldsymbol{k}_1\rangle|^2 \frac{(1-\tau_z)}{2} G(\boldsymbol{k}_1) \frac{(1-\tau_z)}{2} \\ & - \langle \boldsymbol{k}|\boldsymbol{k}_1\rangle\langle -\boldsymbol{k}|-\boldsymbol{k}_1\rangle \frac{(1+\tau_z)}{2} G(\boldsymbol{k}_1) \frac{(1-\tau_z)}{2} \\ & - \langle \boldsymbol{k}|\boldsymbol{k}_1\rangle^*\langle -\boldsymbol{k}|-\boldsymbol{k}_1\rangle^* \frac{(1-\tau_z)}{2} G(\boldsymbol{k}_1) \frac{(1+\tau_z)}{2} \Big].\end{aligned} \tag{A1}$$

In principle, the disorder-averaged scattering potential $\langle V_{\alpha\lambda}(\boldsymbol{k},\boldsymbol{k}_1) V_{\delta\beta}(\boldsymbol{k}_1,\boldsymbol{k})\rangle$ involves integrals of four Bloch eigenstates $\langle \boldsymbol{r},\sigma|k\rangle = u_{\boldsymbol{k}}(\boldsymbol{r};\sigma)$ of the form $v^2 \int d\boldsymbol{r} \sum_{\sigma,\sigma'} u^*_{\boldsymbol{k}'}(\boldsymbol{r};\sigma) u_{\boldsymbol{k}}(\boldsymbol{r};\sigma) u^*_{\boldsymbol{k}}(\boldsymbol{r};\sigma') u_{\boldsymbol{k}'}(\boldsymbol{r};\sigma')$ where the sum over σ implies that the disorder is spatially local spin-independent disorder. Having several subbands occupied in the 1D nanowire, as has recently been proposed,[17,40] should help the situation considerably, both by expanding the regime of stability of the TS phase and by screening out the disorder due to higher carrier density. Substituting the wave function into the matrix elements, we get

$$\begin{aligned}\langle |k|,\theta_{\boldsymbol{k}}||k'|,\theta_{\boldsymbol{k}'}\rangle &\approx \langle k_F,\theta_{\boldsymbol{k}}|k_F,\theta_{\boldsymbol{k}'}\rangle \\ &= \langle 0|e^{i(R_z-\lambda)(\theta_{\boldsymbol{k}}-\theta_{\boldsymbol{k}'})}|0\rangle \\ &= f(\theta_{\boldsymbol{k}}-\theta_{\boldsymbol{k}'}).\end{aligned} \tag{A2}$$

Substituting the matrix elements into the disorder-induced self-energy we find that

$$\begin{aligned}\Sigma(\boldsymbol{k},\omega) = v^2 \int d\boldsymbol{k}_1 \Big[& |f(\theta_{\boldsymbol{k}}-\theta_{\boldsymbol{k}_1})|^2 \frac{[G(\boldsymbol{k}_1)+\tau_z G(\boldsymbol{k}_1)\tau_z]}{2} \\ & - f(\theta_{\boldsymbol{k}}-\theta_{\boldsymbol{k}_1})^2 \frac{(1+\tau_z)}{2} G(\boldsymbol{k}_1) \frac{(1-\tau_z)}{2} \\ & - f(\theta_{\boldsymbol{k}}-\theta_{\boldsymbol{k}_1})^{*2} \frac{(1-\tau_z)}{2} G(\boldsymbol{k}_1) \frac{(1+\tau_z)}{2} \Big].\end{aligned} \tag{A3}$$

To solve Dyson's equations, it is convenient to define the functions $a_{0,z,+,-}(\boldsymbol{k},\omega)$ by the relation

$$\begin{aligned}G^{-1}(\boldsymbol{k},\omega) = & a_0(\boldsymbol{k},\omega) + a_z(\boldsymbol{k},\omega)\tau_z \\ & + a_+(\boldsymbol{k},\omega)\tau_+ + a_-(\boldsymbol{k},\omega)\tau_-.\end{aligned} \tag{A4}$$

Substituting this into the Dyson equations [Eq. (14)] together with the expression for the self-energy [Eq. (A3)] in the lowest order Born approximation we get

$$\begin{aligned}a_0(\boldsymbol{k},\omega) &= \omega - f_0(\pi\tau_{sm})^{-1} \int d\epsilon' \frac{\omega}{\omega^2 - (\epsilon' - \epsilon_{F,sm})^2 - |\Delta|^2}, \\ a_z(\boldsymbol{k},\omega) &= (\epsilon - \epsilon_{F,sm}) + f_0(\pi\tau_{sm})^{-1} \\ &\quad \times \int d\epsilon' \frac{(\epsilon' - \epsilon_{F,sm})}{\omega^2 - (\epsilon' - \epsilon_{F,sm})^2 - |\Delta|^2}, \\ a_+(\boldsymbol{k},\omega) &= \Delta e^{i\theta_{\boldsymbol{k}}} - f_1(\pi\tau_{sm})^{-1} \\ &\quad \times \int d\epsilon' \frac{\Delta e^{i\theta_{\boldsymbol{k}}}}{\omega^2 - (\epsilon' - \epsilon_{F,sm})^2 - |\Delta|^2},\end{aligned} \tag{A5}$$

where $f_0 = \int \frac{d\theta}{2\pi} |f(\theta)|^2$, $f_1 = \int \frac{d\theta}{2\pi} f(\theta)^2 e^{i\theta}$. The integrals in Eq. (A6) can be written analytically as

$$a_0 = \omega + f_0(\pi\tau_{sm})^{-1} \zeta\omega, \tag{A6}$$

$$a_+ = [\Delta + f_1(\pi\tau_{sm})^{-1} \zeta\Delta] e^{i\theta_{\boldsymbol{k}}}, \tag{A7}$$

where

$$\zeta = \int d\epsilon \frac{1}{\epsilon^2 + \Delta^2 - \omega^2} = \frac{\pi}{\sqrt{\Delta^2 - \omega^2}}, \tag{A8}$$

and $a_z(\boldsymbol{k},\omega) = (\epsilon_{\boldsymbol{k}} - \epsilon_{F,sm})$ remains unrenormalized.

The lowest-frequency pole in the disorder-averaged Green's function $G(\boldsymbol{k},\omega)$ given by Eq. (A4), which corresponds to the quasiparticle gap, occurs when $\epsilon_{\boldsymbol{k}} - \epsilon_{F,sm} = a_z = 0$ and $a_0 = |a_+|$. The disorder-averaged quasiparticle gap ω can then be obtained by solving

$$\omega \left[1 + \frac{f_0}{\sqrt{\Delta^2 - \omega^2}} \right] = \Delta \left[1 + \frac{f_1}{\sqrt{\Delta^2 - \omega^2}} \right]. \tag{A9}$$

For sufficiently weak disorder $\tau_{sm}^{-1} \ll \Delta$, the quasiparticle gap $\omega \sim \Delta$, so that we can expand in the reduction of the quasiparticle gap $x = \Delta - \omega$ to lowest order and obtain the quasiparticle gap reduction to be

$$x \sim \frac{\Delta}{2^{1/3}} \left(\frac{(\pi\tau_{sm})^{-1}}{\Delta} \right)^{2/3} (f_0 - f_1)^{2/3}. \tag{A10}$$

This leads to the pole of the disordered-averaged Green's function G which is also the TS state quasiparticle gap in Eq. (17)

$$\omega = \Delta \left[1 - \frac{1}{2^{1/3}} (\pi\tau_{sm}\Delta)^{-2/3} |\langle k_F| - k_F\rangle|^{4/3} \right]. \tag{A11}$$

APPENDIX B: ANALYTIC SOLUTION OF THE SELF-CONSISTENT BORN APPROXIMATION

In this Appendix we provide an exact solution for the quasiparticle gap within the self-consistent Born approximation. To do this, we start with the self-consistent version of Eq. (A6),

$$\begin{aligned} a_0(\boldsymbol{k},\omega) &= \omega - f_0(\pi\tau_{sm})^{-1}\int d\epsilon' \frac{a_0(\boldsymbol{k},\omega)}{a_0(\boldsymbol{k},\omega)^2 - [\epsilon' - a_z(\boldsymbol{k},\omega)]^2 - |a_+(\boldsymbol{k},\omega)|^2}, \\ a_z(\boldsymbol{k},\omega) &= (\epsilon - \epsilon_{F,sm}) + f_0(\pi\tau_{sm})^{-1}\int d\epsilon' \frac{(\epsilon' - \epsilon_{F,sm})}{a_0(\boldsymbol{k},\omega)^2 - [\epsilon' - a_z(\boldsymbol{k},\omega)]^2 - |a_+(\boldsymbol{k},\omega)|^2}, \\ a_+(\boldsymbol{k},\omega) &= \Delta e^{i\theta_k} - f_1(\pi\tau_{sm})^{-1}\int d\epsilon' \frac{a_+(\boldsymbol{k},\omega)}{a_0(\boldsymbol{k},\omega)^2 - [\epsilon' - a_z(\boldsymbol{k},\omega)]^2 - |a_+(\boldsymbol{k},\omega)|^2}. \end{aligned} \tag{B1}$$

Performing the ϵ' integral in the second equation we immediately obtain $a_z(\boldsymbol{k},\omega) = 0$. Performing the ϵ' integral in the other two equations

$$a_0 = \omega + a\frac{a_0}{\sqrt{a_+^2 - a_0^2}}, \tag{B2}$$

$$a_+ = \Delta + b\frac{a_+}{\sqrt{a_+^2 - a_0^2}}, \tag{B3}$$

where the square root is chosen so that the real part of $\sqrt{a_+^2 - a_0^2}$, $a = \pi f_0(\pi\tau_{sm})^{-1}$ and $b = \pi f_1(\pi\tau_{sm})^{-1}$. Writing $y = \sqrt{a_+^2 - a_0^2}$, the pair of equations can be combined to a single equation for y:

$$1 = \frac{\Delta^2}{(y-b)^2} - \frac{\omega^2}{(y-a)^2}. \tag{B4}$$

At $\omega \sim 0$, the equation has four real roots $y \sim a$ and $y \sim b \pm \Delta$. The quasiparticle gap is defined by the value of ω above which the Green's function $G(\omega)$ has a finite imaginary part. This corresponds to the value of ω where two of the real roots of y merge into a pair of complex roots, so that Eq. (B4) has two real and two complex roots. Using the properties of quartic polynomial equations, the transition point between four real roots and two real roots is signaled by the vanishing of the discriminant of the quartic polynomial. Solving for the frequency ω where the discriminant vanishes leads to the solution

$$\omega = \Delta\sqrt{1 - 3g^{2/3}(f_0 - f_1)^{2/3} + 3g^{4/3}(f_0 - f_1)^{4/3} - 3g^2(f_0 - f_1)^2}, \tag{B5}$$

where $g = 1/\pi\Delta\tau_{sm}$. In the 2D Rashba and 1D superconducting case, we get the solution of the TS state quasiparticle gap in Eq. (18)

$$\omega = \Delta[1 - 3(\pi\tau_{sm}\Delta)^{-2/3}|\langle k_F|\,-k_F\rangle|^{4/3} + 3(\pi\tau_{sm}\Delta)^{-4/3}|\langle k_F|\,-k_F\rangle|^{8/3} - 3(\pi\tau_{sm}\Delta)^{-2}|\langle k_F|\,-k_F\rangle|^4]^{1/2}. \tag{B6}$$

*Present address: Department of Physics, Harvard University, Cambridge, Massachusetts 02138, USA.

[1] Jay D. Sau, R. M. Lutchyn, S. Tewari, and S. Das Sarma, Phys. Rev. Lett. **104**, 040502 (2010).

[2] S. Tewari, J. D. Sau, and S. Das Sarma (unpublished).

[3] J. D. Sau, S. Tewari, R. Lutchyn, T. Stanescu, and S. Das Sarma, Phys. Rev. B **82**, 214509 (2010).

[4] R. M. Lutchyn, Jay D. Sau, and S. Das Sarma, Phys. Rev. Lett. **105**, 077001 (2010).

[5] Y. Oreg, G. Refael, and F. von Oppen, Phys. Rev. Lett. **105**, 177002 (2010).

[6] J. Alicea, Phys. Rev. B **81**, 125318 (2010).

[7] L. Mao, M. Gong, E. Dumitrescu, S. Tewari, and C. W. Zhang, e-print arXiv:1105.3483 (to be published).

[8] J. Alicea, Yuval Oreg, Gil Refael, Felix von Oppen, and Matthew P. A. Fisher, Nature Phys. **7**, 412 (2011).

[9] J. D. Sau, S. Tewari, and S. Das Sarma, Phys. Rev. A **82**, 052322 (2010).

[10] F. Hassler, A. R. Akhmerov, C.-Y. Hou, and C. W. J. Beenakker, New J. Phys. **12**, 125002 (2010).

[11] S. Bravyi and A. Kitaev, Phys. Rev. A **71**, 022316 (2005).

[12] J. D. Sau, S. Tewari, and S. Das Sarma, Phys. Rev. B **84**, 085109 (2011).

[13] S. Das Sarma, M. Freedman, and C. Nayak, Phys. Rev. Lett. **94**, 166802 (2005).

[14] S. Das Sarma, C. Nayak, and S. Tewari, Phys. Rev. B **73**, 220502(R) (2006).

[15] L. Fu and C. L. Kane, Phys. Rev. Lett. **102**, 216403 (2009).

[16] A. R. Akhmerov, J. Nilsson, and C. W. J. Beenakker, Phys. Rev. Lett. **102**, 216404 (2009).

[17] T. D. Stanescu, R. M. Lutchyn, and S. Das Sarma, Phys. Rev. B **84**, 144522 (2011); R. M. Lutchyn, T. D. Stanescu, and S. Das Sarma, e-print arXiv:1110.5643 (to be published).

[18] P. W. Brouwer, M. Duckheim, A. Romito, and F. von Oppen, Phys. Rev. Lett. **107**, 196804 (2011).

[19]A. C. Potter and P. A. Lee, Phys. Rev. B **83**, 184520 (2011).
[20]P. W. Brouwer, M. Duckheim, A. Romito, and F. von Oppen, Phys. Rev. B **84**, 144526 (2011).
[21]P. W. Anderson, J. Phys. Chem. Solids **11**, 26 (1959).
[22]B. A. Bernevig and S.-C. Zhang, Phys. Rev. Lett. **95**, 016801 (2005).
[23]R. Winkler, H. Noh, E. Tutuc, and M. Shayegan, Phys. Rev. B **65**, 155303 (2002).
[24]C. W. Zhang, S. Tewari, R. M. Lutchyn, and S. Das Sarma, Phys. Rev. Lett. **101**, 160401 (2008).
[25]M. Sato, Y. Takahashi, and S. Fujimoto, Phys. Rev. Lett. **103**, 020401 (2009).
[26]A. A. Abrikosov, L. P. Gorkov, and I. E. Dzyaloshinski, *Methods of Quantum Field Theory in Statistical Physics* (Dover Publications Inc., New York, 1963).
[27]J. D. Sau, R. M. Lutchyn, S. Tewari, and S. Das Sarma, Phys. Rev. B **82**, 094522 (2010).
[28]Y. Doh, J. A. van Dam, A. L. Roest, E. P. A. M. Bakkers, L. P. Kouwenhoven and S. De Franceschi, Science **309**, 272 (2005).
[29]J. M. Luttinger, Phys. Rev. **102**, 1030 (1956).
[30]J. Xiang, A. Vidan, M. Tinkham, R. M. Westervelt, and C. M. Lieber, Nature Nano. **1**, 208 (2006).
[31]Y. A. Bychkov and E. I. Rashba, J. Phys. C **17**, 6039 (1984).
[32]R. Winkler, Phys. Rev. B **62**, 4245 (2000).
[33]P. Ghosh, J. D. Sau, S. Tewari, and S. Das Sarma, Phys. Rev. B **82**, 184525 (2010).
[34]L. P. Kouwenhoven (private communication).
[35]A. C. Ford, J. C. Ho, Y.-L. Chueh, Y.-C. Tseng, Z. Fan, J. Guo, J. Bokor, and A. Javey, Nano Lett. **9**, 360 (2009).
[36]A. C. Ford, S. Chuang, J. C. Ho, Y.-L. Chueh, Z. Fan, and A. Javey, Nano Lett. **10**, 509 (2010).
[37]X. W. Zhang and J. B. Xia, Phys. Rev. B **74**, 075304 (2006).
[38]E. H. Hwang and S. Das Sarma, Phys. Rev. B **67**, 115316 (2003).
[39]O. Motrunich, K. Damle, and D. A. Huse, Phys. Rev. B **63**, 224204 (2001).
[40]R. M. Lutchyn, T. D. Stanescu, and S. Das Sarma, Phys. Rev. Lett. **106**, 127001 (2011).